Published in final edited form as:
Free Radic Biol Med. 2010 August 15; 49(4): 606–611. doi:10.1016/j.freeradbiomed.2010.05.010.

Uncoupling protein-3 lowers reactive oxygen species production in isolated mitochondria

Laurence J. Toime[a] and **Martin D. Brand**[a,b,*]

[a]Medical Research Council Mitochondrial Biology Unit, Hills Road, Cambridge CB2 0XY, UK

[b]Buck Institute for Age Research, 8001 Redwood Blvd, Novato, CA 94945, USA

Abstract

Mitochondria are the major cellular producers of reactive oxygen species (ROS), and mitochondrial ROS production increases steeply with increased protonmotive force. The uncoupling proteins (UCP1, UCP2 and UCP3) and adenine nucleotide translocase induce proton leak in response to exogenously added fatty acids, superoxide or lipid peroxidation products. "Mild uncoupling" by these proteins may provide a negative feedback loop to decrease protonmotive force and attenuate ROS production. Using wild type and *Ucp3*$^{-/-}$ mice, we found that native UCP3 actively lowers the rate of ROS production in isolated energized skeletal muscle mitochondria, in the absence of exogenous activators. The estimated specific activity of UCP3 in lowering ROS production was 90 to 500 times higher than that of the adenine nucleotide translocase. The mild uncoupling hypothesis was tested by measuring whether the effect of UCP3 on ROS production could be mimicked by chemical uncoupling. A chemical uncoupler mimicked the effect of UCP3 at early time points after mitochondrial energization, in support of the mild uncoupling hypothesis. However, at later time points the uncoupler did not mimic UCP3, suggesting that UCP3 can also affect on ROS production through a membrane potential-independent mechanism.

Keywords

Adenine nucleotide translocase; Membrane Potential; Mitochondria; Reactive Oxygen Species; Uncoupling protein; ANT; UCP3

In cells, mitochondria are the major producers of the reactive oxygen species (ROS) that can result in the oxidative stress and mitochondrial dysfunction found in many age-related and degenerative diseases [1–3]. Different components of the electron transport chain generate ROS under different conditions, although complexes I and III are thought to be amongst the important sites [4]. The rate of ROS production increases steeply with increased protonmotive force [5,6], and it has been hypothesized that partial dissipation of the protonmotive force by mild uncoupling of oxidative phosphorylation is a mechanism used by mitochondria to attenuate ROS production [7,8].

*Corresponding author. M.D. Brand, Buck Institute for Age Research, 8001 Redwood Blvd, Novato, CA 94945, USA. Tel +1 415-493-3676. Fax +1-415-209-2232. mbrand@buckinstitute.org (M.D. Brand)..

The uncoupling proteins (UCPs) and adenine nucleotide translocase (ANT) are members of the mitochondrial carrier family, and can provide regulated pathways for uncoupling [9]. UCP1 is the best characterized of these proteins, mediating non-shivering thermogenesis in brown adipose tissue by catalyzing proton leak activated by long-chain fatty acids and inhibited by purine nucleotides [10]. UCP3 is expressed predominantly in skeletal muscle and brown adipose mitochondria, at concentrations 200–700-fold lower than UCP1 in brown adipose tissue [11]. Its physiological function has remained controversial. Suggested functions include mild uncoupling, for which there is good empirical evidence [1,12,13]. It has also been proposed that UCP3 is involved in increasing fatty acid oxidation, a hypothesis supported primarily by correlative studies and transgenic UCP3-overexpression experiments; however, no impairment in fatty acid oxidation has been found in mice lacking UCP3 [13–17].

The mild uncoupling hypothesis for UCPs proposes that they partially uncouple mitochondria in the presence of ROS or downstream peroxidation products, resulting in a negative feedback loop that decreases ROS production by lowering both the protonmotive force and local oxygen concentration [7,8]. This idea has been supported by several experiments in which UCP3-dependent uncoupling in isolated mitochondria was activated by exogenously generated superoxide or exogenous lipid peroxidation products such as HNE (4-hydroxynonenal) [18–20]. Furthermore, mice lacking UCP3 had increased levels of oxidative damage markers and decreased activity of aconitase, a protein sensitive to damage by superoxide [14,21,22]. However, whether UCP3 functions to attenuate ROS production by simply catalyzing mild uncoupling remains to be directly tested.

In the present study we use wild type (WT) and *Ucp3* knockout (KO) transgenic mice to test the hypothesis that UCP3 lowers ROS production in isolated mitochondria by catalyzing mild uncoupling. We find that native UCP3 actively lowers the rate of ROS production in isolated energized skeletal muscle mitochondria, in the absence of exogenous activators. From estimates of specific activity, UCP3 is 90 to 500 times more effective at lowering ROS production than ANT. We further show that the effect of UCP3 in lowering ROS production can be mimicked by a chemical uncoupler, consistent with a simple uncoupling mechanism for UCP3, although another more complex activity develops over time.

Materials and methods

Animals

Mice were housed at 21 ± 2 °C, 57 ± 5% humidity, 12/12 h light/dark, with standard chow and water ad libitum, following UK Home Office Guidelines for the Care and Use of Laboratory Animals. Male and female *Ucp3* knockout mice (*Ucp3*KO) [23] were crossed 10 times into the C57BL/6 background, and were sacrificed at age 12–15 weeks along with wild type (WT) sex- and sibling-paired controls. *Ucp3* ablation was confirmed by PCR analysis of genomic *Ucp3* and Western blot analysis in skeletal muscle mitochondria.

Mitochondria

Four mice per preparation were killed by stunning followed by cervical dislocation, and mitochondria were isolated from total hind limb skeletal muscle [19]. WT and *Ucp3*KO mitochondria were assayed in parallel in 96-well plates using a fluorescence microplate reader (Spectramax Gemini XPS, Molecular Devices) set at 37°C, which measured fluorescence of each well every 25 s. Mitochondria were suspended at 0.35 mg mitochondrial protein/ml in assay medium comprising 120 mM KCl, 3 mM HEPES, 1 mM EGTA, 5 mM KH_2PO_4, pH 7.2 supplemented with 0.3% (w/v) defatted bovine serum albumin (BSA), 6 U/ml horseradish peroxidase (HRP), 30 U/ml superoxide dismutase

(SOD), 1 μg/ml oligomycin and 80 ng/ml nigericin. Either 50 μM Amplex Red or 5 μM safranin O was included for measurement of H_2O_2 or membrane potential, respectively, and all conditions were measured in triplicate for each independent experiment. The reaction was initiated by addition of 10 mM succinate.

Measurement of H_2O_2 in isolated mitochondria

Mitochondrial H_2O_2 production was measured fluorescently using Amplex Red (Invitrogen) [24]. HRP catalyzed reaction between Amplex Red and H_2O_2, in the presence of exogenously added SOD, to form the fluorophore resorufin, with excitation and emission wavelengths at 563 nm and 587 nm, respectively. H_2O_2 standard curves were generated for each condition for each independent experiment, to calculate the cumulative mitochondrial H_2O_2 production from the resorufin signal at each measurement time point. The rate of H_2O_2 production at each time point was then determined by calculating the rate of change of H_2O_2 concentration over the following two min, in nmol H_2O_2/min/mg mitochondrial protein. Background rates of fluorescence change in the absence of added succinate were very small, but were subtracted for each experiment.

Measurement of membrane potential using safranin O

Mitochondrial membrane potential was measured using the positively charged dye safranin O, which changes fluorescence in a manner linearly proportional to the mitochondrial membrane potential [25]. The safranin O signal for each condition was measured at excitation and emission wavelengths of 533 nm and 576 nm, respectively, before mitochondrial energization with succinate, throughout energization, and then for 10 min after dissipation of the membrane potential by addition of 0.3 μM FCCP (carbonylcyanide *p*-trifluoromethoxyphenylhydrazone). The relative decrease in fluorescent signal upon energization of the mitochondria is proportional to the membrane potential (above about 60 mV), and results are reported as the absolute magnitude of this change in fluorescence, with larger changes in relative fluorescence units (RFU) indicating higher membrane potentials. Comparison of the safranin O signal before energization and after dissipation of the membrane potential with FCCP allowed correction for any small drift in the baseline fluorescent signal.

Statistics

Data shown are means ± SEM. Student's *t*-tests were used as appropriate to compare two averages. Graphpad Prism (Version 5) was used for statistical analysis of data using analysis of variance (ANOVA), to find best-fit regressions, or to test for differences between curves.

Results

Reactive oxygen species (ROS) production by energised skeletal muscle mitochondria from wild type and *UCP3*KO mice

To investigate the role of UCP3 in mitochondrial ROS production, the rate of H_2O_2 production was measured in isolated mouse skeletal muscle mitochondria respiring on succinate in the absence of rotenone. Under these conditions, ROS production rate is high and originates mostly from the Q-binding site of complex I [26]. Over the 10 min course of the assay, *Ucp3*KO mitochondria produced significantly more ROS than WT mitochondria (Fig. 1A). The rate of ROS production by both WT and *Ucp3*KO mitochondria was relatively stable for the first two min after energization, but then decreased by more than 50% over the course of the assay (Fig. 1B). Addition of carboxyatractylate, an inhibitor of fatty acid-mediated proton transport through the adenine nucleotide translocase (ANT), largely eliminated this decrease in ROS production in *Ucp3*KO mitochondria (and also in

WT, not shown), indicating a time-dependent involvement of the ANT in lowering ROS production rates (Fig. 1B). The average ROS production rate over the first two min was 17% higher in *Ucp3*KO mitochondria than in WT mitochondria (Fig. 1C), suggesting a significant role for UCP3 in the regulation of ROS generation. Critically, addition of 500 μM GDP eliminated the difference between WT and *Ucp3*KO mitochondria, indicating that UCP3 was actively lowering ROS production, and that secondary changes in other proteins (such as antioxidant defences) resulting from UCP3 knockout in the mice did not account for the differences in ROS generation between WT and *Ucp3*KO mitochondria. Addition of 500 μM GDP to *Ucp3*KO mitochondria also resulted in a small but non-significant increase in the ROS production rate over the first two min, which was likely due to inhibition of uncoupling through the ANT by GDP.

Activity of UCP3 and ANT in lowering ROS

UCP3 lowered the rate of ROS production by an average 0.0824 ± 0.0002 nmol H_2O_2/min/mg protein over the course of the assay, as shown by the difference between the ROS production rates of WT and *Ucp3*KO mitochondria (Fig. 2). The activity of UCP3 remained relatively stable, even though the overall rate of ROS production was decreasing (Fig. 1B), such that UCP3 had a proportionately greater effect on the rate of ROS production over time, accounting for an average 39% decrease in ROS production 8 to 10 min after energization.

The effect of ANT in lowering ROS production over time is shown in as the difference between *Ucp3*KO H_2O_2 production rates in the presence and absence of carboxyatractylate. These data show that ANT proton transport activity increased steeply over the first five min of energization, before peaking at 0.480 ± 0.005 nmol H_2O_2/min/mg protein. Assuming the abundance of UCP3 is 4 pmol/mg protein [11] and that of ANT is 500-fold higher at 2 nmol/mg protein [27], this implies that each UCP3 molecule was 500 times more effective than ANT at lowering ROS at the start of the assay, and 90 times more effective than fully active ANT later in the assay. This compares well with other studies reporting a 100-fold higher proton conductance of UCP3 than of ANT [20].

What is the mechanism by which UCP3 lowers ROS production?

It has been previously reported that ROS production by the electron transport chain in mitochondria is dependent on the protonmotive force [5]. To test whether UCP3 was mediating changes in ROS production through effects on protonmotive force, the fluorophore Safranin O was used to measure the membrane potential of WT and *Ucp3*KO mitochondria in parallel with the ROS production measurements shown in Fig. 1. Mitochondria lacking UCP3 had a higher membrane potential than those containing UCP3, and addition of GDP acutely eliminated this difference (Fig. 3). These data show that the effect of UCP3 on ROS production correlated with the effect of UCP3 on membrane potential. The absolute fluorescent signal should not be compared between the presence and absence of GDP, as GDP slightly quenched the Safranin O signal.

The mild uncoupling hypothesis predicts that if UCP3 lowers ROS production through a simple uncoupling mechanism, then the simple chemical uncoupler FCCP should mimic the effect of UCP3 on ROS and membrane potential in mitochondria lacking UCP3. To test this prediction, the relationship between ROS production and membrane potential was determined in WT and *Ucp3*KO mitochondria by independently incubating them with different amounts of FCCP. If UCP3 was indeed working by simple uncoupling, then lowering the membrane potential with a particular concentration of FCCP should be equivalent to having UCP3 present in the mitochondria. This would mean that FCCP titrations of WT and *Ucp3*KO mitochondria would generate the same relationship between

ROS production and membrane potential, and the curves should overlay. The rate of ROS production over the first two min after energization was plotted as a function of membrane potential (Fig. 4). In the absence of FCCP, *Ucp3*KO mitochondria had both a higher rate of ROS production and a higher membrane potential than WT mitochondria without FCCP (as also shown in Figures 1C and 3. However, the dotted lines show that addition of 10 nM FCCP to *Ucp3*KO mitochondria resulted in a lowering of both the membrane potential and ROS production rate to that of WT mitochondria without FCCP. This indicates that a simple chemical uncoupler can indeed mimic UCP3. Moreover, all subsequent FCCP titration points in both WT and *Ucp3*KO mitochondria overlay, and exponential or polynomial nonlinear curve fitting (Prism) was unable to distinguish the curves, further demonstrating that FCCP is equivalent to the presence of UCP3 under these conditions. These data show that the observed differences in ROS production between WT and *Ucp3*KO mitochondria can be completely explained by differences in membrane potential. They support the hypothesis that UCP3 lowers ROS production through a simple uncoupling mechanism in the first two min after energization, although other mechanisms by which the presence of UCP3 alters membrane potential (such as alterations in the activity of substrate oxidation) are not excluded by this experiment.

Chemical uncouplers cannot fully account for UCP3 activity

Although UCP3 had a constant effect on ROS production over the 10-min time course (Fig. 2), the ability of GDP to inhibit this activity decreased over time. Fig. 5A shows that 8–10 min after energization, GDP caused an increase in both WT and *Ucp3*KO ROS production rates, but was unable to eliminate the difference between WT and *Ucp3*KO ROS production. It has previously been demonstrated that GDP can inhibit ANT-dependent proton flux [28,29]; thus it is likely that the increase in ROS production in *Ucp3*KO mitochondria treated with GDP was primarily due to inhibition of ANT. The mechanism through which GDP increases ROS production rates in *Ucp3*KO mitochondria was further investigated using carboxyatractylate to prevent proton leak through the ANT. It was found that there was no significant difference between ROS production rates in the presence of both GDP and carboxyatractylate, and rates in the presence of carboxyatractylate alone (data not shown). Carboxyatractylate has no known target other than the ANT [30], suggesting that GDP was mediating the bulk of its effect in *Ucp3*KO mitochondria through partial inhibition of the ANT.

Despite not inhibiting UCP3-dependent decreases in ROS production 8–10 min after energization, GDP was still effective in eliminating UCP3-dependent decreases in membrane potential (Fig. 5B), suggesting that UCP3 was no longer lowering ROS production solely through a simple uncoupling mechanism. This is further supported by Fig. 5C, which shows the rate of ROS production 8–10 min after energization, plotted as a function of membrane potential. The dotted lines show that at a given membrane potential, WT and *Ucp3*KO mitochondria now produced ROS at different rates, and that the WT and *Ucp3*KO FCCP titrations are now best modelled as separate curves ($P<0.001$, Prism). This indicates that FCCP was no longer able to mimic the presence of UCP3.

Discussion

We provide clear evidence that UCP3 can actively lower ROS production in isolated skeletal muscle mitochondria respiring on succinate, and that it does so in a manner that can be mimicked by the simple chemical uncoupler FCCP. UCP-dependent activity over the first 2 min after energization was inhibited by GDP, which eliminated differences in both membrane potential and ROS production, and indicated that UCP3 was acutely and actively lowering ROS production rates.

UCP3 was endogenously activated under our assay conditions, and its activity remained constant with time, in contrast to previous results showing that UCP3 is activated gradually over the first 5 min after energization [29]. One possible explanation for this difference is the presence of rotenone (which inhibits the high levels of superoxide produced at complex I during reverse electron transport) in [29] but not in the present experiments. The faster rate of ROS production here could greatly increase the rate at which UCP3 activators, such as HNE, are produced, giving more rapid endogenous activation of UCP3.

The effect of GDP on increasing ROS production rates in *Ucp3*KO mitochondria is consistent with previous studies showing that GDP is not a specific inhibitor of UCP3 [28,29]. Our results also suggest that the most of the non-UCP3 effect of GDP is mediated through the ANT, although an effect of GDP on other mitochondrial carriers cannot be ruled out.

The ability of FCCP to mimic the presence of UCP3 at early time points after energization is consistent with the mild uncoupling hypothesis, suggesting that UCP3 is able to lower ROS production through a simple uncoupling mechanism. However, ROS production is not a unique function of membrane potential, depending also on other variables such as the redox state of ubiquinone in the electron transport chain, which was not measured in this study. Therefore, these data do not eliminate alternative explanations for the effect of UCP3 on ROS production; for example, the possibility that UCP3 affects ubiquinone redox state in a manner distinct from simple uncoupling.

At later time points after energization with succinate, GDP eliminated significant differences in membrane potential; however, UCP3 was still able to lower the ROS production rate. FCCP was unable to mimic UCP3 activity at these later time points, suggesting that UCP3 is able to manifest a difference in ROS production rate through a membrane potential-independent mechanism. This GDP- and membrane potential-independent mechanism is activated gradually after energization, and thus could occur due to the build-up of activating species, such as lipid peroxidation products. The membrane potential-independent mechanism by which UCP3 is able to lower ROS production is unclear; however, possible explanations include UCP3 working to export highly reactive fatty acid peroxides. It is also possible that UCP3 may export superoxide directly to cytochrome *c*, where it can be safely oxidized in a process that regenerates protonmotive force [31].

We found that UCP3 had a specific activity in lowering ROS production 90–500 times higher than the related mitochondrial carrier protein ANT, and that UCP3 was activated to the maximum extent found in this assay much earlier after energization than was ANT. These observations are consistent with the hypothesis that uncoupling proteins may act as a first line of defence against ROS generated by the electron transport chain in conditions of high oxidative damage, for example by helping to attenuate further ROS production after ischaemia-reperfusion events.

Acknowledgments

We thank the Medical Research Council (UK), National Institutes of Health (USA) grants P01 AG025901, PL1 AG032118 and P30 AG025708 and Keck Foundation for financial support. We also thank Julie Buckingham, Helen Boysen, Nadeene Parker and Adrian Lambert for their technical assistance.

Abbreviations

ANT	adenine nucleotide translocase
BSA	bovine serum albumin

CAT	carboxyatractylate
FCCP	carbonylcyanide-*p*-trifluoromethoxyphenylhydrazone
HNE	4-hydroxynonenal
HRP	horseradish peroxidase
ROS	reactive oxygen species
SOD	superoxide dismutase
UCP	uncoupling protein.

References

[1]. Brand MD, Affourtit C, Esteves TC, Green K, Lambert AJ, Miwa S, Pakay JL, Parker N. Mitochondrial superoxide: production, biological effects, and activation of uncoupling proteins. Free Radic. Biol. Med. 2004; 37:755–767. [PubMed: 15304252]

[2]. Raha S, Robinson BH. Mitochondria, oxygen free radicals, disease and ageing. Trends Biochem. Sci. 2000; 25:502–508. [PubMed: 11050436]

[3]. Ambrosio G, Zweier JL, Duilio C, Kuppusamy P, Santoro G, Elia PP, Tritto I, Cirillo P, Condorelli M, Chiariello M, et al. Evidence that mitochondrial respiration is a source of potentially toxic oxygen free radicals in intact rabbit hearts subjected to ischemia and reflow. J. Biol. Chem. 1993; 268:18532–18541. [PubMed: 8395507]

[4]. St-Pierre J, Buckingham JA, Roebuck SJ, Brand MD. Topology of superoxide production from different sites in the mitochondrial electron transport chain. J. Biol. Chem. 2002; 277:44784–44790. [PubMed: 12237311]

[5]. Korshunov SS, Skulachev VP, Starkov AA. High protonic potential actuates a mechanism of production of reactive oxygen species in mitochondria. FEBS Lett. 1997; 416:15–18. [PubMed: 9369223]

[6]. Liu Y, Chen L, Xu X, Vicaut E, Sercombe R. Both ischemic preconditioning and ghrelin administration protect hippocampus from ischemia/reperfusion and upregulate uncoupling protein-2. BMC Physiol. 2009; 9:17. [PubMed: 19772611]

[7]. Papa S, Skulachev VP. Reactive oxygen species, mitochondria, apoptosis and aging. Mol. Cell. Biochem. 1997; 174:305–319. [PubMed: 9309704]

[8]. Brand MD. Uncoupling to survive? The role of mitochondrial inefficiency in ageing. Exp. Gerontol. 2000; 35:811–820. [PubMed: 11053672]

[9]. Affourtit C, Crichton PG, Parker N, Brand MD. Novel uncoupling proteins. Novartis Found. Symp. 2007; 287:70–80. discussion 80–91. [PubMed: 18074632]

[10]. Nicholls DG, Locke RM. Thermogenic mechanisms in brown fat. Physiol. Rev. 1984; 64:1–64. [PubMed: 6320232]

[11]. Harper JA, Stuart JA, Jekabsons MB, Roussel D, Brindle KM, Dickinson K, Jones RB, Brand MD. Artifactual uncoupling by uncoupling protein 3 in yeast mitochondria at the concentrations found in mouse and rat skeletal-muscle mitochondria. Biochem. J. 2002; 361:49–56. [PubMed: 11743882]

[12]. Brand MD, Buckingham JA, Esteves TC, Green K, Lambert AJ, Miwa S, Murphy MP, Pakay JL, Talbot DA, Echtay KS. Mitochondrial superoxide and aging: uncoupling-protein activity and superoxide production. Biochem. Soc. Symp. 2004:203–213. [PubMed: 15777023]

[13]. Bezaire V, Seifert EL, Harper ME. Uncoupling protein-3: clues in an ongoing mitochondrial mystery. FASEB J. 2007; 21:312–324. [PubMed: 17202247]

[14]. Vidal-Puig AJ, Grujic D, Zhang CY, Hagen T, Boss O, Ido Y, Szczepanik A, Wade J, Mootha V, Cortright R, Muoio DM, Lowell BB. Energy metabolism in uncoupling protein 3 gene knockout mice. J. Biol. Chem. 2000; 275:16258–16266. [PubMed: 10748196]

[15]. Costford SR, Chaudhry SN, Salkhordeh M, Harper ME. Effects of the Presence, Absence and Overexpression of Uncoupling Protein-3 on Adiposity and Fuel Metabolism in Congenic Mice. Am. J. Physiol. Endocrinol. Metab. 2006

[16]. Hoeks J, Hesselink MK, Sluiter W, Schaart G, Willems J, Morrisson A, Clapham JC, Saris WH, Schrauwen P. The effect of high-fat feeding on intramuscular lipid and lipid peroxidation levels in UCP3-ablated mice. FEBS Lett. 2006; 580:1371–1375. [PubMed: 16455084]

[17]. Himms-Hagen J, Harper ME. Physiological role of UCP3 may be export of fatty acids from mitochondria when fatty acid oxidation predominates: an hypothesis. Exp. Biol. Med. (Maywood). 2001; 226:78–84. [PubMed: 11446442]

[18]. Echtay KS, Roussel D, St-Pierre J, Jekabsons MB, Cadenas S, Stuart JA, Harper JA, Roebuck SJ, Morrison A, Pickering S, Clapham JC, Brand MD. Superoxide activates mitochondrial uncoupling proteins. Nature. 2002; 415:96–99. [PubMed: 11780125]

[19]. Echtay KS, Esteves TC, Pakay JL, Jekabsons MB, Lambert AJ, Portero-Otin M, Pamplona R, Vidal-Puig AJ, Wang S, Roebuck SJ, Brand MD. A signalling role for 4-hydroxy-2-nonenal in regulation of mitochondrial uncoupling. EMBO J. 2003; 22:4103–4110. [PubMed: 12912909]

[20]. Parker N, Vidal-Puig AJ, Brand MD. Stimulation of mitochondrial proton conductance by hydroxynonenal requires a high membrane potential. Biosci. Rep. 2008

[21]. Brand MD, Pamplona R, Portero-Otin M, Requena JR, Roebuck SJ, Buckingham JA, Clapham JC, Cadenas S. Oxidative damage and phospholipid fatty acyl composition in skeletal muscle mitochondria from mice underexpressing or overexpressing uncoupling protein 3. Biochem. J. 2002; 368:597–603. [PubMed: 12193161]

[22]. Talbot DA, Brand MD. Uncoupling protein 3 protects aconitase against inactivation in isolated skeletal muscle mitochondria. Biochim. Biophys. Acta. 2005; 1709:150–156. [PubMed: 16084485]

[23]. Gong DW, Monemdjou S, Gavrilova O, Leon LR, Marcus-Samuels B, Chou CJ, Everett C, Kozak LP, Li C, Deng C, Harper ME, Reitman ML. Lack of obesity and normal response to fasting and thyroid hormone in mice lacking uncoupling protein-3. J. Biol. Chem. 2000; 275:16251–16257. [PubMed: 10748195]

[24]. Zhou M, Diwu Z, Panchuk-Voloshina N, Haugland RP. A stable nonfluorescent derivative of resorufin for the fluorometric determination of trace hydrogen peroxide: applications in detecting the activity of phagocyte NADPH oxidase and other oxidases. Anal. Biochem. 1997; 253:162–168. [PubMed: 9367498]

[25]. Akerman KE, Wikstrom MK. Safranine as a probe of the mitochondrial membrane potential. FEBS Lett. 1976; 68:191–197. [PubMed: 976474]

[26]. Lambert AJ, Brand MD. Inhibitors of the quinone-binding site allow rapid superoxide production from mitochondrial NADH:ubiquinone oxidoreductase (complex I). J. Biol. Chem. 2004; 279:39414–39420. [PubMed: 15262965]

[27]. Brand MD, Pakay JL, Ocloo A, Kokoszka J, Wallace DC, Brookes PS, Cornwall EJ. The basal proton conductance of mitochondria depends on adenine nucleotide translocase content. Biochem. J. 2005; 392:353–362. [PubMed: 16076285]

[28]. Khailova LS, Prikhodko EA, Dedukhova VI, Mokhova EN, Popov VN, Skulachev VP. Participation of ATP/ADP antiporter in oleate- and oleate hydroperoxide-induced uncoupling suppressed by GDP and carboxyatractylate. Biochim. Biophys. Acta. 2006

[29]. Parker N, Affourtit C, Vidal-Puig AJ, Brand MD. Energisation-dependent endogenous activation of proton conductance in skeletal muscle mitochondria. Biochem. J. 2008

[30]. Klingenberg M. The ADP and ATP transport in mitochondria and its carrier. Biochim Biophys Acta. 2008; 1778:1978–2021. [PubMed: 18510943]

[31]. Pereverzev MO, Vygodina TV, Konstantinov AA, Skulachev VP. Cytochrome c, an ideal antioxidant. Biochem. Soc. Trans. 2003; 31:1312–1315. [PubMed: 14641051]

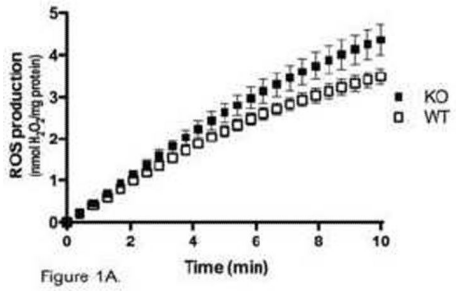

Figure 1A.

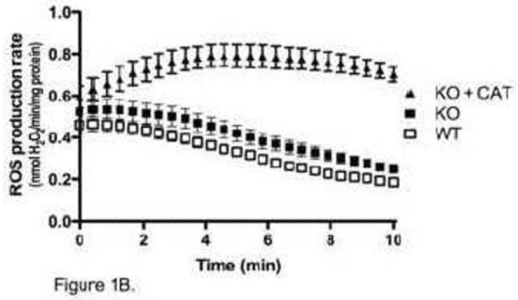

Figure 1B.

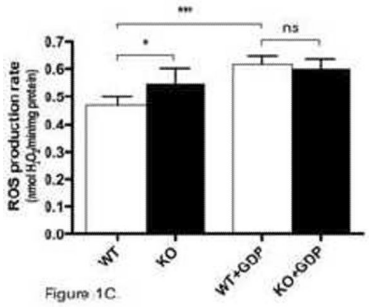

Figure 1C.

Figure 1. Rate of ROS production in WT and *Ucp3*KO skeletal muscle mitochondria

The rate of H_2O_2 production was measured in WT and *Ucp3*KO skeletal muscle mitochondria as described in Materials and Methods. **(A)** The cumulative amount of ROS produced is shown over 10 min after energization with succinate. **(B)** The rate of ROS production is shown over 10 min after energization with succinate. 2.5 μM carboxyatractylate (CAT) was present as indicated. **(C)** The average rate of ROS production calculated over the first 2 min after energization with succinate, with or without 500 μM GDP. Values are means ± SEM of triplicate experiments performed on 9 separate preparations. One-way ANOVA was performed for **(C)**, with Tukey's multiple comparison test used comparing the bars: **P*<0.05, ****P*<0.001

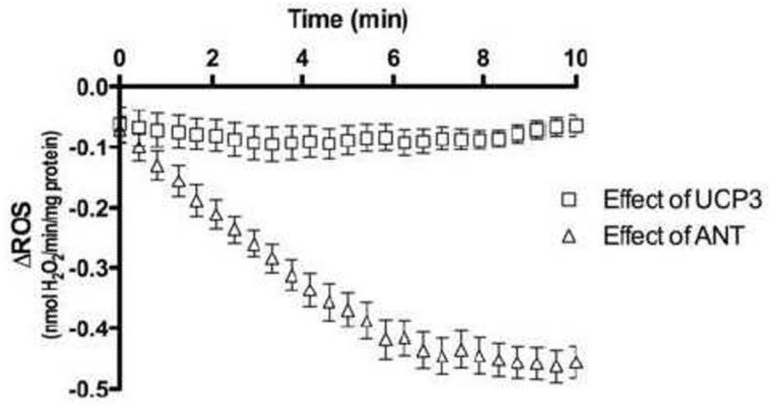

Figure 2. Effect of UCP3 and ANT in lowering ROS production

The effect of UCP3 on ROS production was calculated for each time point after energization with succinate by subtracting the rate of ROS production in *Ucp3*KO mitochondria from the rate in WT mitochondria. The effect of ANT was calculated in *Ucp3*KO mitochondria by subtracting the rate of ROS production in the presence of 2.5 μM CAT from the rate without CAT.

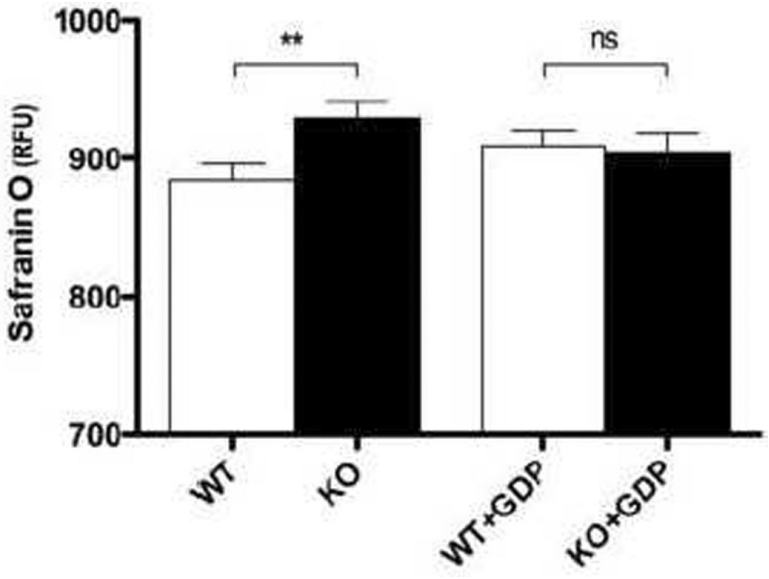

Figure 3. Effect of UCP3 on membrane potential 0–2 min after energization

The membrane potential was measured in WT and *Ucp3*KO skeletal muscle mitochondria over the first two min after energization, as described in Materials and Methods. Values are means ± SEM of triplicate experiments performed on 9 separate preparations.

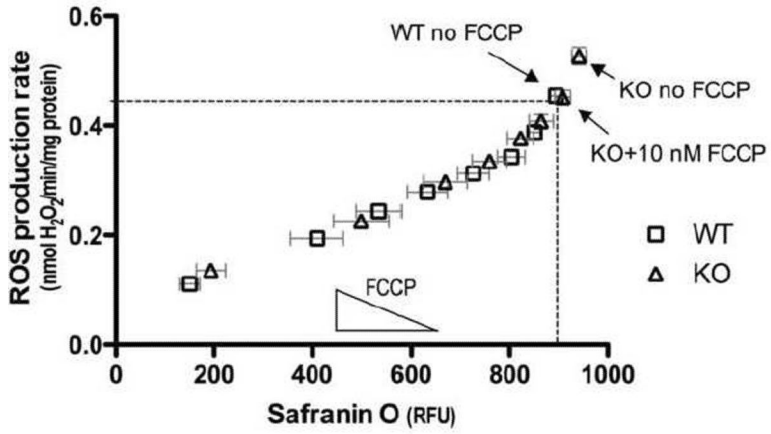

Figure 4. FCCP can mimic the effect of UCP3 on ROS production and membrane potential 0–2 min after energization

Mitochondria from WT and *Ucp3*KO mice were independently energized with different amounts of FCCP from 0–60 nM. ROS production rates over the first 2 min are plotted against average membrane potential over the same period. Nonlinear regression analysis (Prism) using exponential and polynomial models found that a single curve best describes the data in all cases. Dashed lines highlight the ROS production rate and membrane potential for WT mitochondria without FCCP, and for *Ucp3*KO mitochondria in the presence of 10 nM FCCP. Values are means ± SEM of triplicate experiments performed on 11 separate preparations.

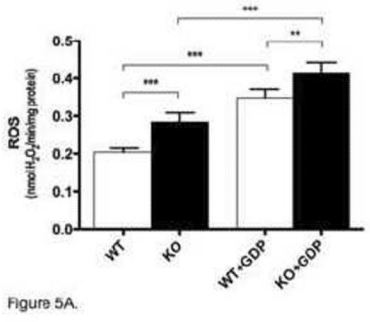

Figure 5A.

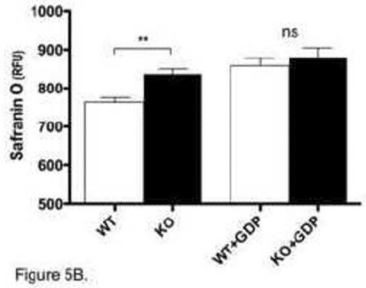

Figure 5B.

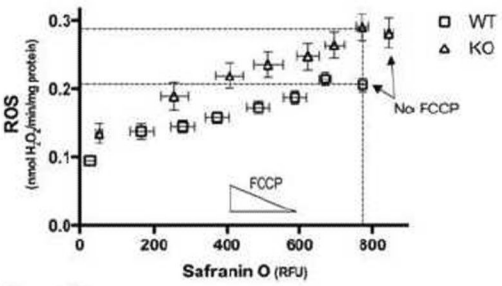

Figure 5C.

Figure 5. Effect of UCP3 in skeletal muscle mitochondria 8–10 min after energization

(A) The average rate of ROS production in WT and *Ucp3*KO mitochondria was measured 8–10 min after energization, with or without 500 μM GDP. **(B)** The average membrane potential in WT and *Ucp3*KO mitochondria was measured 8–10 min after energization, with or without 500 μM GDP. **(C)** Mitochondria from WT and *Ucp3*KO mice were independently energized with different amounts of FCCP from 0–60 nM. ROS production rates over 8–10 min after energization are plotted against average membrane potential over the same period. Linear and nonlinear regression analysis (Prism) show that the data are best modelled by two different curves ($P<0.0001$). Dashed lines highlight the ROS production rate and membrane potential for WT mitochondria without FCCP, and for *Ucp3*KO mitochondria in the presence of 10 nM FCCP. Values are means ± SEM of triplicate experiments performed on 9 (**A, B**) or 11 (**C**) separate preparations.